

PATTERNS AND PROCESSES IN THE DISTRIBUTION AND DYNAMICS OF ANTARCTIC KRILL

S.A. Levin, A. Morin and T.M. Powell

Abstract

A general framework is presented to develop, test and integrate component models of the distribution and dynamics of Antarctic krill population at various spatial and temporal scales. We suggest that models of increasing complexity be developed iteratively for variability and patchiness of krill abundance. Incremental models should then be compared to statistical descriptions of the observed distribution patterns at various scales of observation to ascertain the plausibility of the model and identify critical processes to be added. An analysis of spatial distribution of krill in the Bransfield Strait area reveals that purely physical models of turbulent redistribution are not sufficient to explain krill distribution at small scales. We therefore propose to develop a modified diffusion-reaction model incorporating spatially variable growth rates of krill, krill loss rates due to predators, and density-dependent attraction of krill to account for the small-scale aggregations.

Résumé

Une structure générale est présentée afin de développer, de tester et d'intégrer des modèles constitutifs de la répartition et de la dynamique de la population du krill antarctique à différentes échelles spatiales et temporelles. Nous suggérons que soient développés d'une manière itérative des modèles de complexité croissante portant sur la variabilité et la répartition irrégulière de l'abondance du krill. Des modèles incrémentiels devraient ensuite être comparés aux descriptions statistiques des formes de répartition observées à différentes échelles d'observation afin de déterminer la plausibilité du modèle et d'identifier les processus critiques à ajouter. Une analyse de la répartition spatiale du krill dans la région de détroit de Bransfield montre que des modèles purement physiques de redistribution turbulente ne suffisent pas à expliquer la répartition du krill à de petites échelles. Nous proposons donc de développer un modèle modifié de diffusion-réaction incorporant les taux de croissance du krill variables sur le plan spatial, les taux de perte de krill due aux prédateurs, et l'attraction du krill en fonction de la densité pour expliquer les concentrations sur une petite échelle.

Резюме

Представлена общая схема разработки, опробования и интеграции однокомпонентных моделей распределения и динамики популяции антарктического криля по различным пространственным и временным масштабам. Мы предлагаем, чтобы возрастающей сложности модели многообразия и неравномерности распространения криля

разрабатывались итеративно, появляющиеся вновь модели должны затем сравниваться со статическим описанием наблюдавшихся картин распределения по различным масштабам, по которым проводились наблюдения, чтобы оценить степень достоверности модели и выявить ключевые процессы, требующие включения в модель. Анализ пространственного распределения криля в районе пролива Брансфилда показал, что чисто физической модели турбулентного перераспределения криля недостаточно для объяснения мелкомасштабного распределения криля. В связи с этим для того, чтобы объяснить существование небольших агрегаций криля, мы предлагаем разработать диффузно-реактивную модель, включающую также и пространственные переменные - такие, как темпы роста криля, смертность криля, зависящая от хищников, и взаимное привлечение криля, обусловленное плотностью скопления.

Resumen

Se presenta una estructura general a fin de desarrollar, analizar e integrar los modelos componentes de la distribución y dinámica de la población de krill antártico a distintas escalas espaciales y temporales. Se sugiere la elaboración de modelos de creciente complejidad en forma iterativa para la variabilidad y discontinuidad de la abundancia de krill. Se deberá comparar luego los modelos de incremento con las descripciones estadísticas de los patrones de distribución obtenidos a distintas escalas de observación para establecer la plausibilidad del modelo e identificar los procesos críticos que deban agregarse. Un análisis de la distribución espacial de krill en el área del estrecho de Bransfield revela que los modelos puramente físicos de redistribución turbulenta no son suficientes para explicar la distribución del krill a pequeñas escalas. Por consiguiente se propone desarrollar un modelo modificado de reacción-difusión que incorpore los índices de crecimiento del krill de variación espacial, los índices de pérdidas del krill a causa de predadores, la atracción de krill dependiente de la densidad para explicar el porqué de las concentraciones a pequeña escala.

1. INTRODUCTION

Among the important questions being addressed in scientific studies of living marine resources in the Antarctic are:

1. How important are physical processes, such as the movement of fronts and sea-surface contiguous zones, in determining the distribution and dynamics of krill and fin fish?
2. How important are biological factors such as predation and food availability?
3. What is the interaction between spatial patterns and fishing behavior?
4. How can theoretical approaches to stock assessment and prediction facilitate the estimation of the size of the resource, and aid in the development of optimal harvesting strategies?

In the Antarctic ecosystems, as in other complex ecosystems, physical and biological factors interact to produce patterns of multiple spatial and temporal scales. The initial steps in the development of a quantitative theory of the Antarctic must involve an examination of those scales (Denman and Powell, 1984; Levin, 1988). Spectral analysis and other statistical approaches allow comparison of observed distributions of physical factors, primary producers, and consumers; mechanistic investigations provide complementary information on natural time and space scales for biological and physical processes underlying patterns.

In the equatorial mid-Pacific, over the 2-50 km spatial scales, the range for which the best data are available for comparison with the Antarctic ecosystem, estimation of fractal dimensions of phytoplankton patches suggests that physical factors are the primary determinants of spatial pattern (Slice et al., 1988). Of course, it is quite a leap from the equatorial ocean to the Antarctic, but spectral analyses of data from the Southern Ocean lead to the same conclusion. We turn in the next section to an examination of the evidence. The implications are substantial, since if the proposition is accepted, it means that primary productivity can be modelled as, to a first approximation, a reflection of physical conditions.

2. DISTRIBUTION OF TEMPERATURE AND FLUORESCENCE

In various data sets taken from different regions of the Antarctic, the concordance between physical factors (temperature) and primary productivity (fluorescence) is excellent on intermediate and broader scales. Figure 1, reprinted from Weber et al. (1986), demonstrates the similarity of slopes in the spectral distributions of temperature and fluorescence in the Southern Ocean in austral summer 1981; the middle panels in Figure 2 indicate strong coherence in the distributions. Weber et al. (1986) believe that the slightly steeper slope of the fluorescence spectrum, plus the strong coherence between fluorescence and krill (Figure 2), is evidence that grazing is a factor in the small-scale distribution of phytoplankton. We are not convinced, and in any case, regard physical factors as providing an adequate explanation of the fluorescence spectrum at least on intermediate scales (4-20 km). It is unfortunate that we do not yet have available comparable data for the Elephant Island-Bransfield Strait region. We hope to be able to obtain such data to strengthen our interpretation of krill distributions, reported in the next section.

Our conclusion is that, to a first approximation, it is reasonable to regard phytoplankton abundance as determined by physical processes. Of course, this is based entirely on correlations; nonetheless, it is our null hypothesis. In our modelling approach,

this assumption will represent our baseline model. In later versions of the model, grazing will be allowed to modify the basic distribution.

3. PRELIMINARY DATA ANALYSIS OF KRILL SPATIAL DISTRIBUTION

Quantitative descriptions of krill spatial distribution are necessary for two purposes. The first is that the patterns revealed by those descriptions allow the formulation of the simplest models that can reproduce these properties. The second reason is that the descriptions of real spatial distributions will serve as standards to which to compare the output of the candidate models.

The most useful analyses to date are those of Weber et al. (1986) discussed in the previous section and shown in Figures. 1 and 2, for the spatial distributions of temperature, fluorescence, and krill biomass in the Antarctic Ocean south of Africa. The power spectra for temperature and fluorescence, shown in Figure 1 and discussed in the last section, differ markedly from that reported for krill biomass. The variance of fluorescence and temperature declines with increasing wavenumber (decreasing wavelength). The slope of the relationship between the log variance and the log wavenumber approaches previously reported values for these quantities (Powell et al., 1975; Mackas, 1977; Steele and Henderson, 1977; Lekan and Wilson, 1978; Platt and Denman, 1980); these slopes were close to the $-5/3$ prediction of Kolmogorov (1941) for the inertial subrange of turbulence. In contrast, the krill power spectrum was almost flat, indicating an approximately equal variance at all scales.

The description of Weber et al. (1986) implies that different mechanisms control temperature and fluorescence spatial distributions on the one hand, and krill distribution on the other. As suggested in the previous section, purely physical models may be sufficient to explain fluorescence spatial distribution (at least in the 2-20 km length scales of the Weber et al. study). However, such a model could not reproduce the krill spectral estimates; additional mechanisms must be invoked.

If the description of Weber et al. (1986) were to hold for the Elephant Island-Bransfield Strait region, it could serve as the basis for a preliminary model of that region. The submodel for primary productivity of algal biomass distribution would be primarily physical. The close correspondence of the spectral estimates for temperature and fluorescence suggests that grazing by herbivores has a minimal effect on algal spatial distribution. In contrast, a purely physical model for krill would be inappropriate since it could not produce the relatively high variability at small scales (high wavenumber). Although krill distribution undoubtedly is influenced by physical processes (such as advection and turbulence), other factors (presumably involving krill behavior) must be responsible for the high heterogeneity at small scales. Thus, a krill submodel would have to include additional mechanisms acting predominantly at small scales.

The first step of this analysis was to examine, through spectral analysis, the krill biomass distribution in the vicinity of King George Island and then to compare the resulting power spectrum to the description of Weber et al. (1986) to determine whether the same type of spectrum can describe the krill distribution patterns in different areas.

Acoustic data (provided by M.C. Macaulay), obtained 4-5 January 1987, aboard the RV *Professor Siedlecki*, were analyzed in the following way. The data tapes contained continuous reading of estimated average krill biomass (g m^{-3} ; 200 kHz estimates) at each meter of depth (range: 3-185 m) at a horizontal resolution of approximately 200 m for eight transects (Figure 3). Vertical profiles were summed to obtain an areal estimate of krill biomass (g m^{-2}). The resulting traces were then subdivided into 16 series of 64 data points to be analyzed by spectral analysis. The power at each frequency for the 16 transects

then was summed, and normalized to the total power of the signal to obtain a normalized power spectrum (Figure 4).

To facilitate comparison with the power spectrum of Weber et al. (1986), we also analyzed the data by first averaging areal biomass into 1 km bins, and subdividing the resulting series into traces of 20 data points. The power estimates then were treated as above to obtain an average power spectrum spanning the same scales as Weber et al. (Figure 5).

The resulting spectra (Figures. 4-5) were closely similar to the published spectra for krill, but much less steep than that which commonly has been observed for fluorescence, salinity and temperature. There is a relatively high variability of krill biomass at small scales that apparently cannot be explained by physical processes alone.

A second descriptor of spatial distribution, the semivariogram (see for example, Mackas, 1984), also was computed from the same data (Figure 6). The results indicate that the variability in krill biomass between pairs of data points is only a weak function of the linear distance between those points. The semivariance of log biomass does not vary significantly over most distances between points except for the smallest distances. This suggests that patch size (swarm size) is smaller than 200 m, the finest resolution of those data.

A third, simple descriptor, the *frequency distribution* of biomass, was computed for the same data set (Figure 7). The resulting frequency distribution is bimodal and appears to be the mixture of two lognormal distributions. About two-thirds of the observations (67%) can be attributed to the first lognormal distribution (mean \log_{10} (biomass) = 0.18, SD = 0.49), and one-third to a second lognormal distribution (mean = 1.76, SD = 0.51). These two distributions may correspond to the between- and within-patch biomass (mean biomass between patches = 2.8 g m⁻², apparent mean biomass within patches = 115 g m⁻²). Note that the biomass within swarms may be substantially higher since it appears that most swarms have a diameter smaller than 200 m, and that the observed biomass is an average for a 200 m trace.

4. COMPARISON OF DATA WITH THE PHENOMENOLOGICAL MODEL PREDICTIONS OF MANGEL

As an example of how we intend to use these descriptions to evaluate the plausibility and adequacy of our models, we have reconstructed the "patch within patch" model of Mangel (1987) with minor modification to account for the low "background" biomass of krill. This model assumes that individual krill aggregate in swarms in surface densities of the order of 300 g/m², over a surface spatial extent on the order of 100 m. Swarms of krill are further aggregated into concentrations or patches over a large spatial extent of the order of 10 nautical miles (=20 km). A concentration with a length scale of 15 nautical miles is assumed to have 8000 swarms of krill, randomly placed within the concentration.

Transect data, similar to those analyzed above, were then extracted from the simulated krill spatial distribution, and the three descriptors calculated for 100 sets of 16 transects of 64 points. The results are presented in Figure 8. Not surprisingly, the resulting frequency distribution (Figure 8a) is similar to the one observed for the real data. The semivariogram (Figure 8b) also is both qualitatively and quantitatively similar to the one obtained from real data. The power spectrum of simulated data (Figure 8c) also approximates the one observed for the real data, though it does not mimic the apparent curvature of Figure 4, especially at small scales. Overall, the simple model of Mangel appears to reproduce excellently the patterns observed with real krill biomass data. Of course, this model is phenomenological rather than mechanistic; it is useful as a descriptor

of observed patterns, and for evaluating the success of different fishing and sampling strategies. It does not provide a means of relating patterns to underlying processes.

Obviously, a larger set of real data needs to be analyzed not only to produce more precise descriptions, but also to test whether the power spectra, semivariograms, and/or frequency distributions vary in a systematic fashion among the various subareas of the general Bransfield Strait-Elephant Island area. The same descriptors have to be obtained from the other relevant parameters of the integrated model: temperature, salinity, algal biomass, and density of krill predators.

5. DEVELOPMENT OF A PROCESS-BASED MODEL

Statistical analyses, such as those reported in the previous section, are a start, but are limited as devices for prediction. Without some understanding of mechanisms, we have no idea why correlations hold, or when they will fail (e.g., Lehman, 1986). Therefore, we seek to go beyond such statistical analyses, developing mechanistic explanations of observed patterns.

Our basic approach is built upon modification of classical diffusion reaction models. However, that basic approach must be modified in a number of ways to take into account what is known about mechanisms. Thus, we alter the diffusion-reaction model so that:

1. Krill growth rates are spatially variable functions of phytoplankton availability;
2. Krill loss rates are functions of predator abundance;
3. On broad scales, the assumption of diffusion is replaced by the inertial subrange of turbulence;
4. On smaller scales, the assumption of diffusion is replaced for krill by models for aggregation, such as Kawasaki's (1978) model for long-range density-dependent attraction (see Morin et al., 1989).

6. MODEL IMPLEMENTATION

The integrated spatial and temporal model outlined in the previous section relies on a large number of parameters that presently are unknown. The present data base does not suffice to formulate the model in a more quantitative form. Although the final model may require estimates of most of the parameters, we suggest using an iterative approach in the development of working models.

In the first approximation, we still will assume that the physics determines the distribution and abundance of algae, and that krill distribution depends on algal availability. We further assume that krill consume an insignificant fraction of algal biomass, and that predators have a negligible effect on detailed versions of the model. For the first approximation, the driving forces thus will be found in the hydrographic data. The output of such a model will be compared to real data, both by looking at the large-scale distribution of krill obtained by the acoustic surveys and at the three spatial distribution descriptors (power spectra, semivariogram, frequency distribution), for temperature (or salinity), algal biomass, and krill. Discrepancies between the observed and simulated patterns will indicate the major inadequacies of this simplistic model. It already is apparent that such a model will not reproduce krill distribution adequately, although it is less clear whether it will mimic its temporal variability.

The next (and improved) versions of the model will depend on the results of the first iteration. The second iteration will incorporate the krill aggregation model of Kawasaki and Okubo, and more detailed functions for the encounter rates. Subsequent iterations will include the grazing effect of predation by invertebrates, fish, and marine mammals.

REFERENCES

- DENMAN, K.L. and T.M. POWELL. 1984. Effects of physical processes on planktonic ecosystems in the coastal ocean. *Oceanography and Marine Biology Annual Review* 22: 125-168.
- KAWASAKI, K. 1978. Diffusion and the formation of spatial distribution. *Mathematical Science* 183: 47-52.
- KOLMOGOROV, A. 1941. The local structure of turbulence in incompressible viscous fluid for very large Reynolds' numbers. *Comptes rendus de l'academie des sciences de l'URSS* 32: 16-18.
- LEHMAN, J.T. 1986. The goal of understanding in limnology. *Limnology and Oceanography* 31: 1160-1166.
- LEKAN, J.F. and R.E. WILSON. 1978. Spatial variability of phytoplankton biomass in the surface water of Long Island. *Estuarine and Coastal Marine Science* 6: 239-250.
- LEVIN, Simon A. 1989. Physical and Biological Scales, and the Modeling of Predator-prey Interactions in Large Marine Ecosystems. In: SHERMAN, Kenneth and L.M. ALEXANDER(Eds.). *Patterns, Processes, and Yields of Large Marine Ecosystems*. American Association for the Advancement of Science Selected Symposium. (In press). Chapter 17.
- MACKAS, D.L. 1977. Horizontal spatial variability and covariability of marine phytoplankton and zooplankton. PhD dissertation. Dalhousie University, 220 pp.
- MACKAS, D.L. 1984. Spatial autocorrelation of plankton community composition in a continental shelf ecosystem. *Limnology and Oceanography* 29: 451-471.
- MANGEL, M. 1987. Simulation of southern ocean krill fisheries. SC-CAMLR-VII/BG/22, Report for Commission for the Conservation of Antarctic Marine Living Resources (CCAMLR), 13 October. 86 pp.
- MORIN, Antoine, Akira OKUBO and Kohkichi KAWASAKI. 1988. Acoustic data analysis and models of krill spatial distribution. Background paper for Annual Meeting of Commission for the Conservation of Antarctic Marine Living Resources (CCAMLR), October, Hobart, Tasmania, Australia.
- PLATT, T. and K.L. DENMAN. 1980. Patchiness in phytoplankton distribution. In: MORRIS, I. (Ed.). *The Physiological Ecology of Phytoplankton*. Oxford: Blackwell. pp. 413-431.
- POWELL, T.M., P.J. RICHESON, T.M. DILLON, B.A. AGEE, B.J. DOZIER, D.A. GODDEN, and L.O. MYRUP. 1975. Spatial scales of current speed and phytoplankton biomass fluctuations in Lake Tahoe. *Science* 189: 1088-1090.
- SLICE, D., A. OKUBO, and G. FELDMAN. 1988. Scale-dependent structure of open-ocean plankton patch boundaries. Submitted.

STEELE, J.H. and E.W. HENDERSON. 1977. Plankton patches in the northern North Sea. In: STEELE, J.H. (Ed.). Fisheries Mathematics. New York: Academic Press. pp. 1-19.

WEBER, L.H., S.Z. EL-SAYED, and I. HAMPTON. 1986. The variance spectra of phytoplankton, krill and water temperature in the Antarctic Ocean south of Africa. Deep-Sea Research 33 (10): 1327-1343.

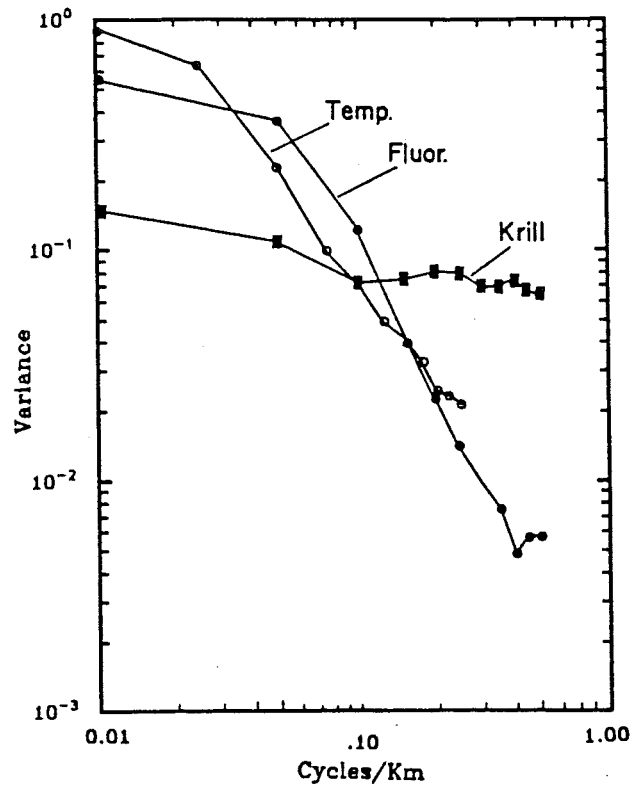


Figure 1: Mean spectral plots for krill, *in vivo* fluorescence, and temperature. (From Weber et al., 1986).

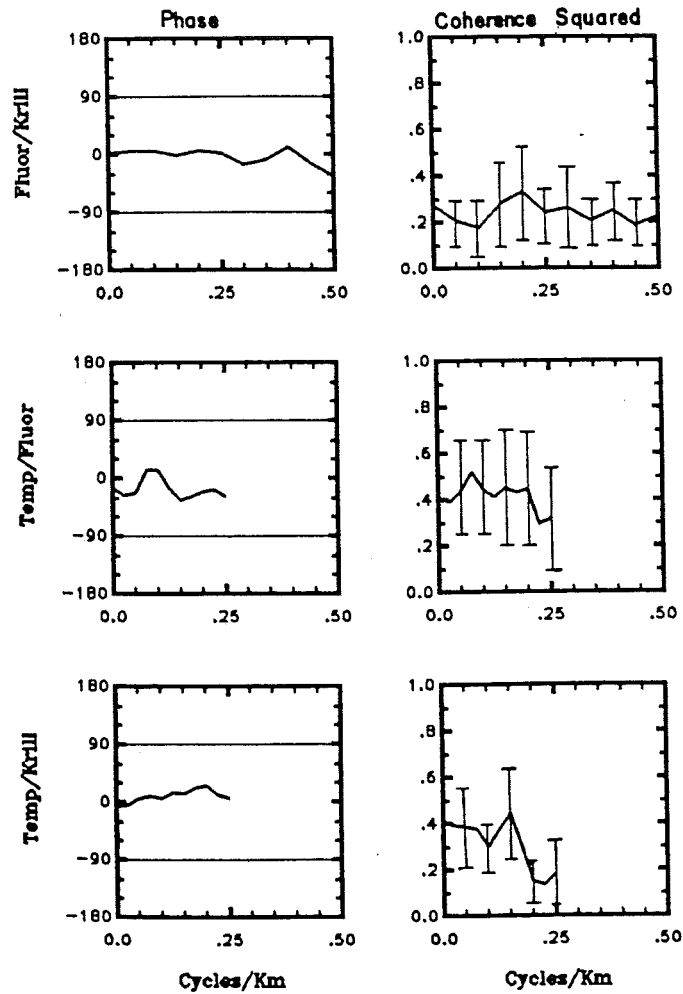


Figure 2: Mean phase and squared coherence spectra for fluorescence-krill, temperature-fluorescence, and temperature-krill. Vertical bars indicate the 95% confidence limits about the mean coherence squared estimates ($\bar{y} \pm (2.2) (S.D. \sqrt{12})$). For clarity, confidence limits for temp-fluor and temp-krill are only shown at every other computed frequency. (From Weber et al., 1986).

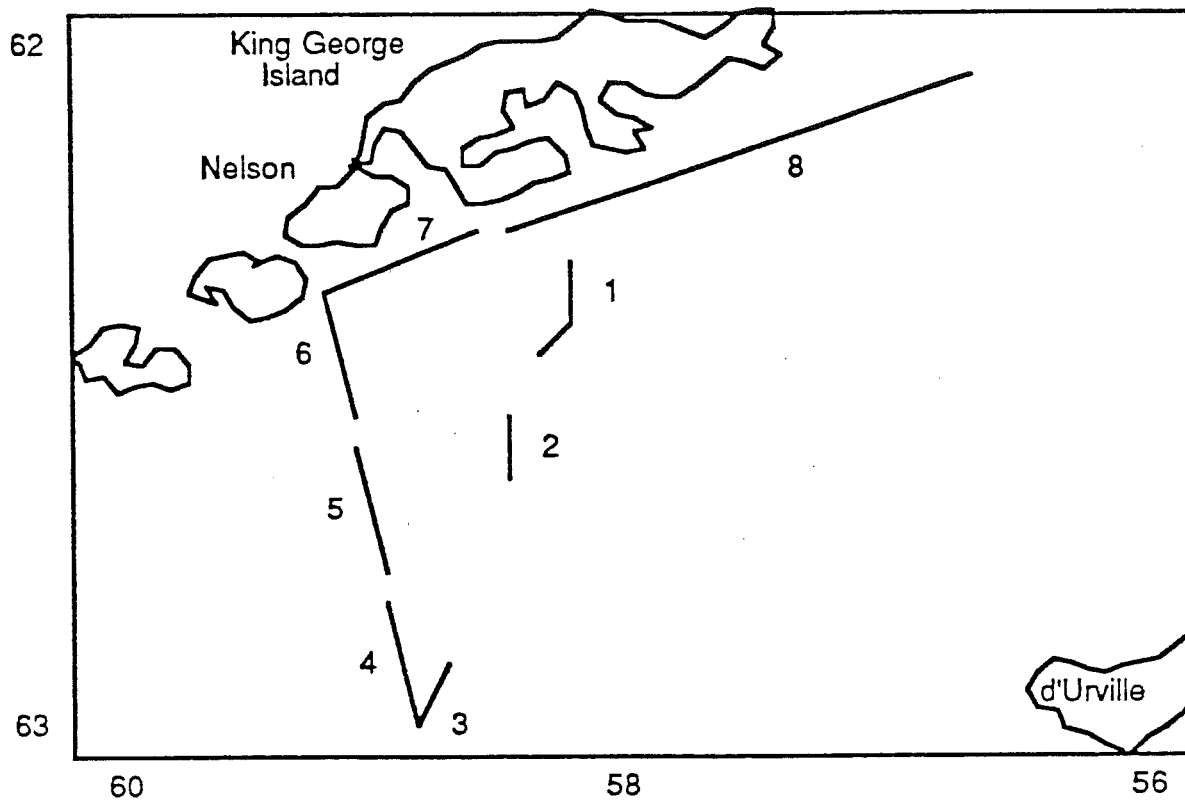


Figure 3: Location of the transects used in the preliminary data analysis. 4-5 January 1987.

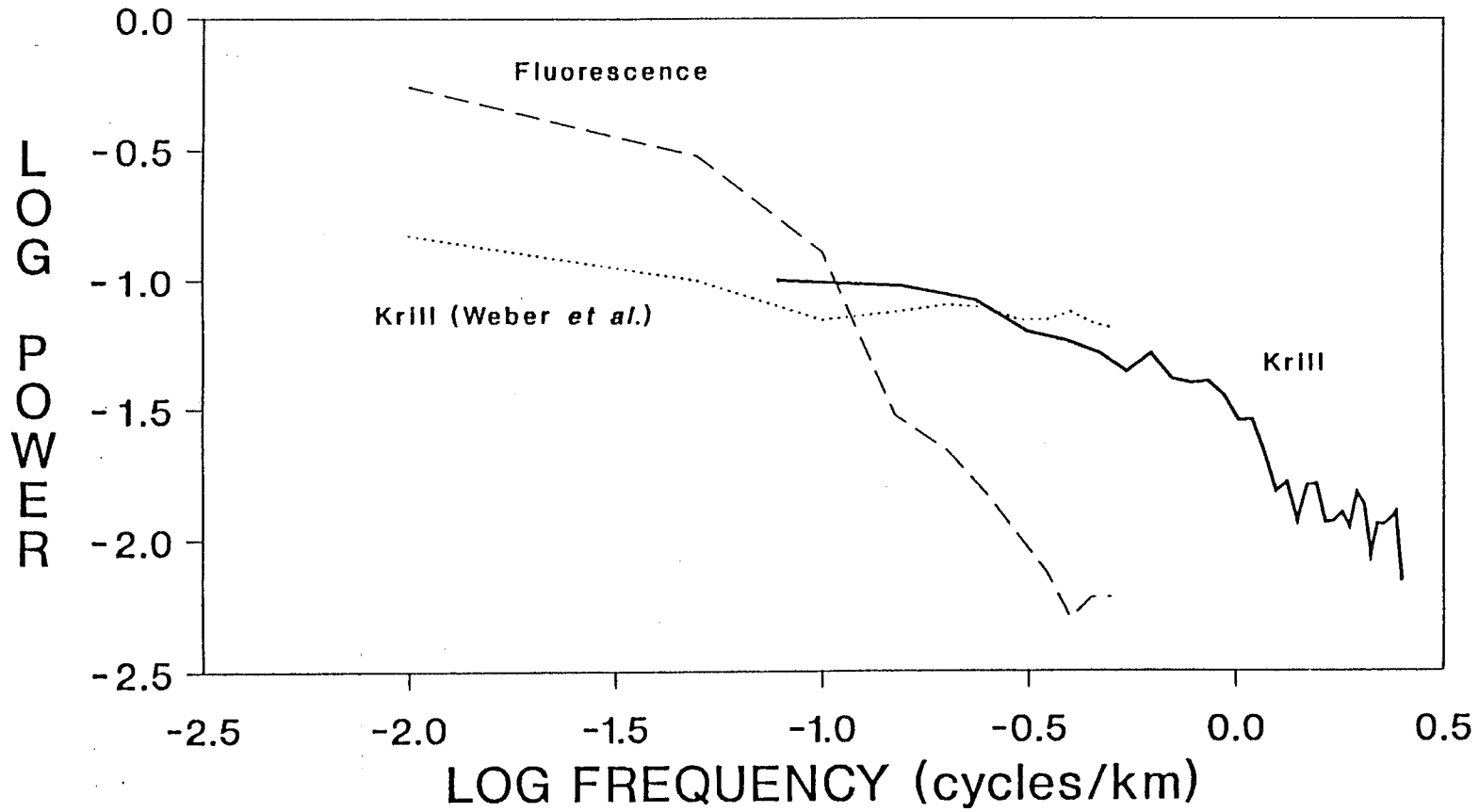


Figure 4: Normalized power spectra of Weber et al. (1986) for fluorescence and krill, compared to the observed spectra for the krill acoustic data.

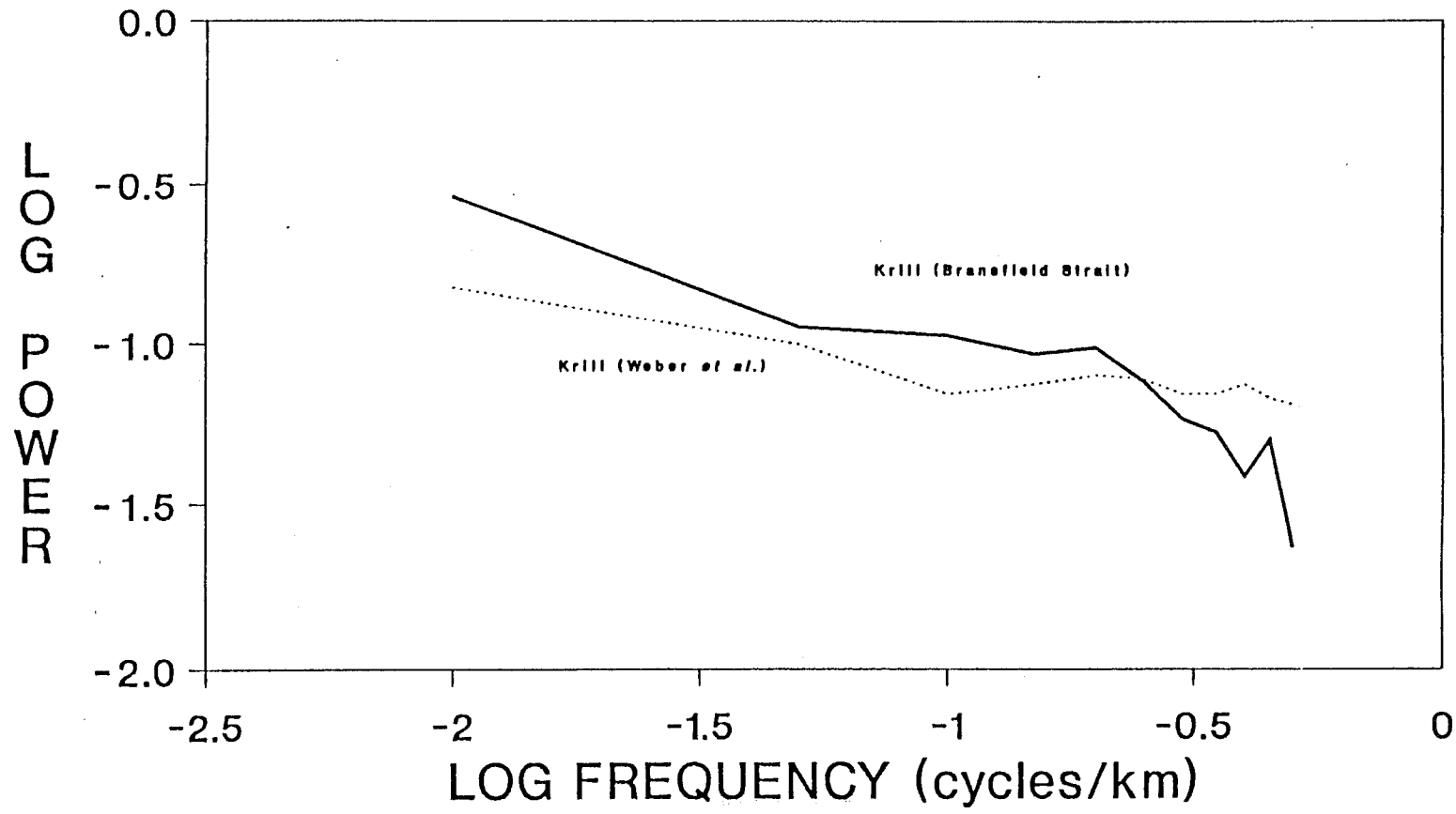


Figure 5: Power spectra for krill at the 2-20 km scale observed in this analysis and by Weber et al. (1986). Krill biomass was averaged over 1 km.

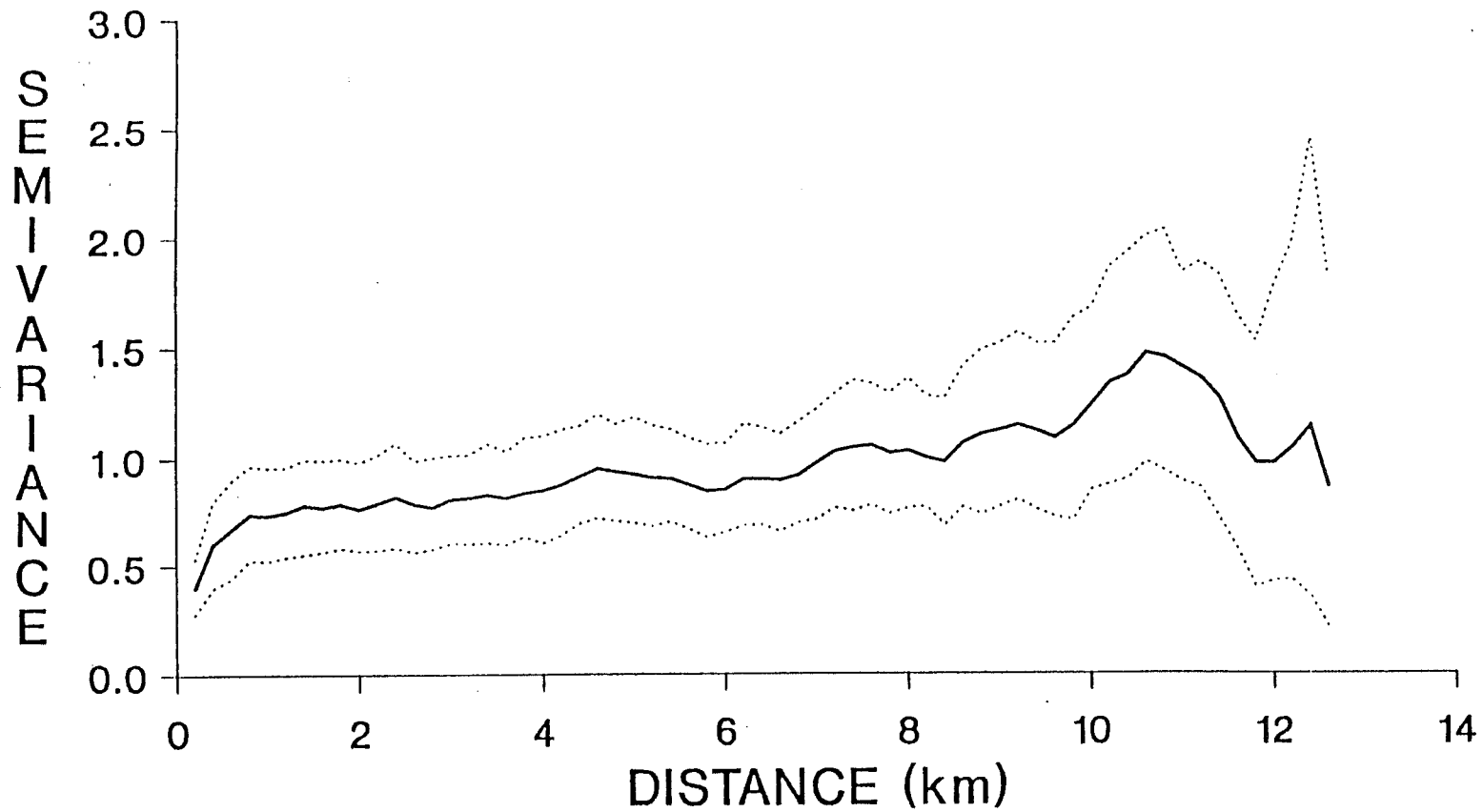


Figure 6: Semivariogram of \log_{10} krill biomass (g/m^2) with bootstrap 95% confidence intervals for the Bransfield Strait data (4-5 January 1987).

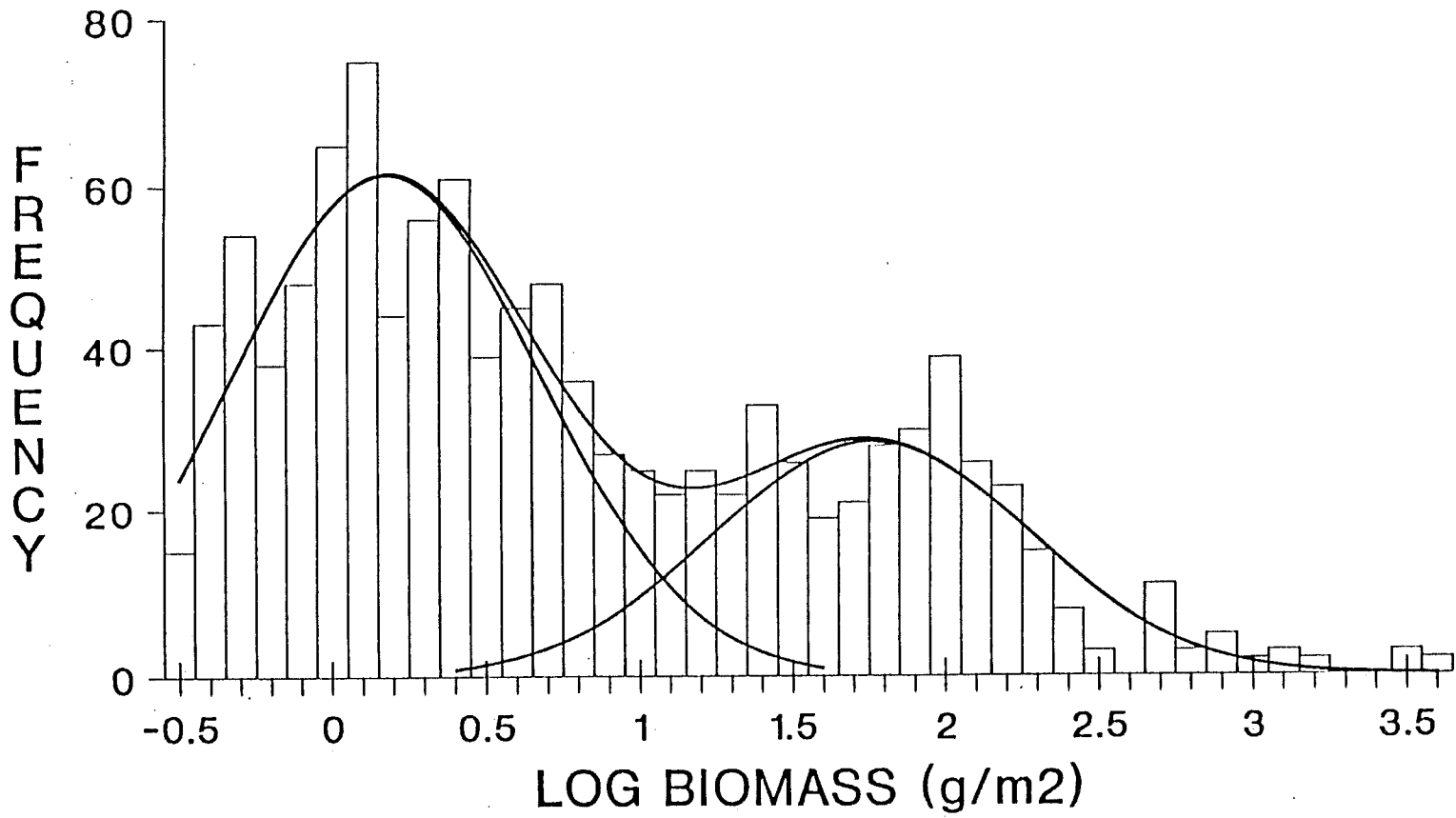
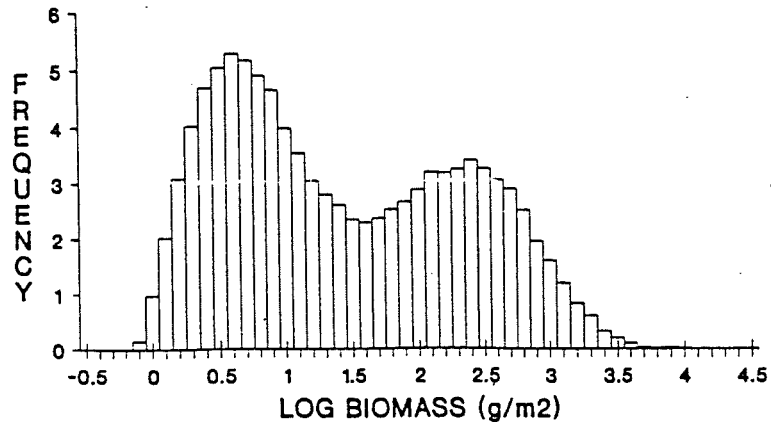
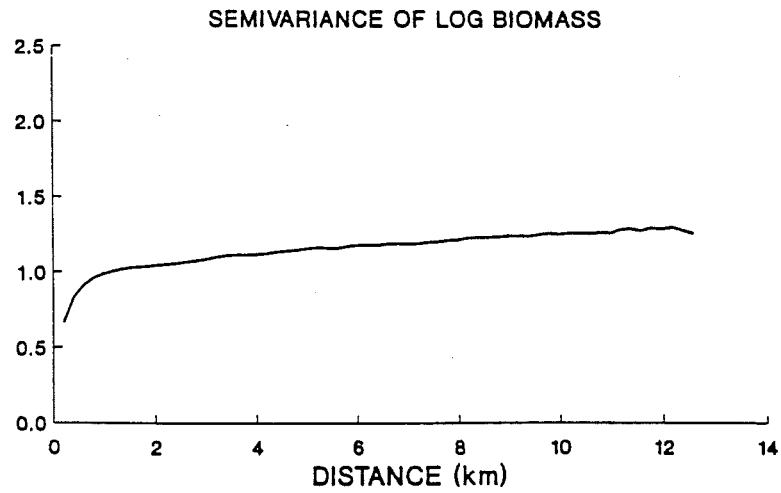


Figure 7: Frequency distribution of \log_{10} biomass estimates (g/m^2) for the Bransfield Strait data (4-5 January 1987).

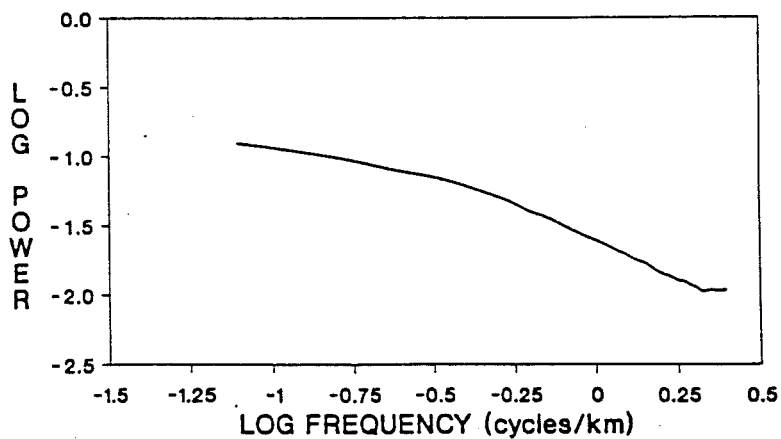
"Patch within patch" model of Mangel



a



b



c

Figure 8: Frequency distribution (a), semivariogram (b), and power spectrum (c) of simulated data using the "patch within patch" model of Mangel (1987).

Лéгeндeс дeс фигурe

- Figure 1 Corrélations spectrales moyennes du krill, de la fluorescence *in vivo*, et de la température. (De Weber et al., 1986).
- Figure 2 Spectres de phase transversale moyenne et cohérence carrée de fluorescence-krill, température-fluorescence, et température-krill. Les barres verticales indiquent les limites de fiabilité de 95% en ce qui concerne les calculs carrés de cohérence moyenne ($\bar{y} \pm (2.2) (S.D.\sqrt{12})$). Afin d'être clair, les limites de fiabilité de température-fluor et de température-krill ne sont montrés qu'à une fréquence calculée sur deux. (De Weber et al., 1986).
- Figure 3 Emplacement des transects utilisés pour les analyses de données préliminaires. 4-5 janvier 1987.
- Figure 4 Spectres normalisés d'intensité de Weber et al. (1986) pour la fluorescence et le krill, et spectres observés des données acoustiques sur le krill analysées.
- Figure 5 Spectres d'intensité du krill sur une échelle de 2-20 km observée dans cette analyse et par Weber et al. La moyenne de la biomasse du krill a été prise sur 1 km.
- Figure 6 Semivariogramme de la biomasse du krill $\log_{10} (g/m^2)$ avec une zone d'intervalles de confiance de 95% pour les données recueillies dans le détroit de Bransfield (4-5 janvier 1987).
- Figure 7 Distribution de fréquences d'estimations \log_{10} de la biomasse (g/m^2) pour les données recueillies dans le détroit de Bransfield (4-5 janvier 1987).
- Figure 8 Distribution de fréquences (a), semivariogramme (b), et spectre d'intensité (c) de données simulées utilisant le modèle de "regroupements à l'intérieur de regroupements" de Mangel (1987).

Подписи к рисункам

- Рисунок 1 Спектральные графики средних величин для криля, *in vivo* флуоресценции и температуры (по Веберу и др., 1986 г.).
- Рисунок 2 Спектры средней кросс-фазовой и квадратичной когерентности для соотношений флуоресценция-криль, температура-флуоресценция, и температура-криль. Вертикальные полосы указывают на доверительные пределы, касающиеся оценок средней квадратичной когерентности ($\bar{y} \pm (2.2) (S.D.\sqrt{12})$). Для ясности, доверительные пределы для соотношений температура-флуоресценция и температура-криль указываются только на каждой второй вычисленной частоте. (по Веберу и др., 1986 г.).
- Рисунок 3 Расположение гидрографических разрезов, использованных при анализе предварительных данных. 4-5 января 1987 г.

- Рисунок 4 Нормализованная спектральная мощность частотного распределения для флуоресценции и криля, по Веберу и др. (1986 г.), и полученные путем наблюдения спектры для проанализированных акустических данных по крилю.
- Рисунок 5 Полученная (Вебером и др.) путем наблюдения в этом анализе спектральная мощность частотного распределения для криля по шкале 2-20 км. Биомасса криля была усреднена по километровому квадрату.
- Рисунок 6 Семивариограмма с логарифмической шкалой (\log_{10}) биомассы криля ($\text{г}/\text{м}^2$) с зоной доверительного интервала (95%) для данных по проливу Брансфилда (4-5 января 1987 г.).
- Рисунок 7 Распределение частоты с логарифмической шкалой (\log_{10}) оценок биомассы ($\text{г}/\text{м}^2$) для данных по проливу Брансфилда (4-5 января 1987 г.).
- Рисунок 8 Распределение частоты (а), семивариограмма (b), и спектральная мощность частотного распределения (с) смоделированных данных при использовании модели Мангела "пятна в пределах пятен" (1987 г.).

Leyenda de la Figura

- Figura 1 Curvas espectrales promedio para el krill, fluorescencia *in vivo* y temperatura. (Weber et al., 1986).
- Figura 2 Frase-cruzada promedio y espectro de coherencia cuadrada para el krill-fluorescencia, fluorescencia-temperatura, y krill-temperatura. Las barras verticales indican los límites de confianza del 95% de las estimaciones promedio de la coherencia cuadrada ($\bar{y} \pm (2.2) (S.D. \sqrt{12})$). Para mayor claridad, los límites de confianza para el flúor-temperatura y krill-temperatura se indican solamente en las frecuencias computadas alternas. (Weber et el., 1986).
- Figura 3 Localización de los transectos utilizados en los análisis de los datos preliminares. 4-5 enero de 1987.
- Figura 4 Densidad espectral normalizada de Weber et al. (1986) para fluorescencia y krill, y espectro observado para los datos acústicos analizados del krill.
- Figura 5 Densidad espectral para el krill en la escala de 2-20 km observada en este análisis y por Weber et al. La biomasa del krill fue calculada por término medio sobre 1 km.
- Figura 6 Semivariograma del \log_{10} de la biomasa del krill (g/m^2) con zonas de intervalos de confianza del 95% para los datos del estrecho de Bransfield (4-5 de enero de 1987).
- Figura 7 Distribución de la frecuencia del \log_{10} de estimaciones de la biomasa (g/m^2) para los datos del estrecho de Bransfield (4-5 de enero de 1987).

Figura 8

Distribución de la frecuencia (a), semivariogram (b), y densidad espectral (c) de los datos simulados usando el modelo de Mangel "mancha dentro de mancha" (1987).